Image-based aircraft pose estimation: a comparison of simulations and real-world data

Marcel G. Breuers, N de Reus

TNO Physics and Electronics Laboratory,
P.O. Box 96864, 2509 JG The Hague, The Netherlands

1. ABSTRACT

The problem of estimating aircraft pose information from mono-ocular image data is considered using a Fourier descriptor based algorithm. The dependence of pose estimation accuracy on image resolution and aspect angle is investigated through simulations using sets of synthetic aircraft images. Further evaluation shows that good pose estimation accuracy can be obtained in real world image sequences.

Keywords: Fourier descriptors, pose estimation, computer vision, target recognition

2. INTRODUCTION

In order to use air defence artillery effectively against incoming aircraft, it is necessary to make accurate predictions of aircraft trajectories. Traditionally, systems capable of pointing and tracking use only position measurements based on radar data to update trajectory estimates. The performance of these systems becomes poor when confronted with fast manoeuvring targets. It is known from literature[1,2] that fusion of target *position* data gathered by radar and target *pose* estimates extracted from camera images results in improved tracking and prediction performance. The fusion process is shown in Figure 1.

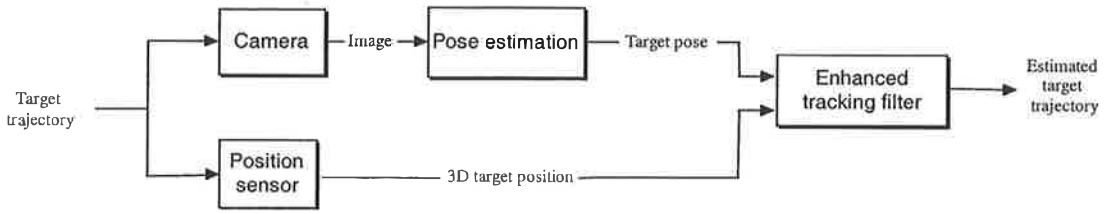

Figure 1. Pose estimation as a part of an enhanced target tracking system.

In this paper we discuss the design, implementation, and testing of an algorithm capable of extracting aircraft pose information from camera images. First, a short introduction to pose estimation techniques is given. Next, the details of the implemented pose estimation algorithm are explained. Finally, the results from simulations and real-world experiments are discussed.

Most methods of image based aircraft pose estimation are based on a two step approach. In the first step of this approach, global rotation, translation, and scale invariant image features are used to compute the aircraft rotation about two axes that are perpendicular to the optical axis of the camera. In the second step, global translation and scale invariant image features are used to compute the aircraft rotation about the optical axis of the camera. This two step strategy is the basis of our pose estimation algorithm.

Moments and Fourier descriptors are the feature types that are predominantly used in aircraft pose estimation. An evaluation of a moment based pose estimation technique indicates that a large fraction of the pose estimation errors can be attributed to poor performance in discriminating between mirrored object shapes[3]. Fourier descriptors are expected to overcome these problems. In this paper we focus on an analysis of the Fourier Descriptor (FRD) based pose estimation method that was introduced by Wallace and Wintz[5].

M. G. J. Breuers and N. de Reus,
Image-based aircraft pose estimation: a comparison of simulations and real-world data,
in F. A. Sadjadi, editor, Proc. of SPIE Vol. 4379, Automatic Target Recognition XI, Orlando (FL), USA, Apr. 2001

Fourier descriptors are feature vectors that can be used to characterize the contour of an object. A Fourier descriptor consists of the *normalized* Fourier transform of the object contour pixel coordinates. The normalization procedure is chosen such that the FRD remains invariant under image scaling, translation and rotation. In addition, the normalization procedure is necessary to make the FRD independent of the pixel sequence starting point on the object contour.

3. THE FRD BASED POSE ESTIMATION ALGORITHM

The structure of the implemented pose estimation algorithm is visualized in figure 2. The processing steps that take place in the conversion from input image to pose estimate are described below.

1 **Object extraction**

The grayscale image from a camera is converted to a binary image by means of thresholding. It is assumed that the aircraft silhouette contains sufficient information for object pose estimation. In addition we assume that only one target is visible in the image and that sufficient contrast between target and background is available to allow for simple and robust image segmentation.

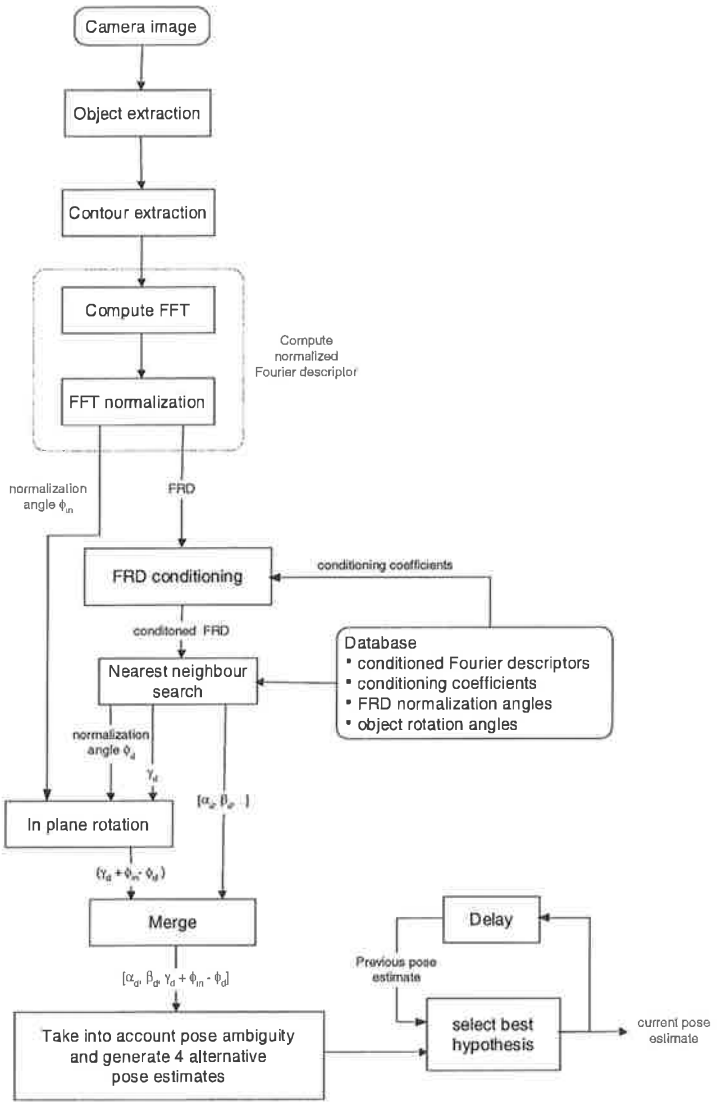

Figure 2. Data flow in the pose estimation algorithm

2 **Contour extraction**
A chain of contour points is extracted from the object. The number of boundary points is converted to a default value by means of linear interpolation.

3. **Compute Fourier descriptor**
The x- and y-coordinates of the object contour are combined into a complex number sequence. A FFT is applied to the sequence to obtain a set of Fourier coefficients. The Fourier coefficients are normalized to obtain an FRD that is independent of the contour starting point. In the same normalization procedure, the object contour is rotated to a default orientation. The *FRD normalization rotation angle* is denoted ϕ_{in}.

4. **FRD conditioning**
The FRD descriptor can be thought of as a feature vector. Often, the performance of pattern recognition techniques can be improved by conditioning the feature vectors. Before conditioning can be applied, the complex valued elements in a FRD vector of size N are transformed into a new feature vector of length 2N. The first N coefficients in the new vector are equal to the real part of the original vector and the coefficients N+1 through 2N are equal to the imaginary part of the original vector. Conditioning may include applying offset and scaling to each vector element to obtain vector element distributions with mean value equal to zero, and variance equal to one. In addition, the use of a Karhunen-Loeve transform can sometimes improve pattern recognition performance. Conditioning and KL-transform are optional steps in the algorithm.

5. **Nearest neighbour search**
The conditioned FRD is compared to a reference database, using the Euclidean distance metric. The results from this search procedure are the best matching FRD in the database, the corresponding database aircraft orientation, denoted $[\alpha_d, \beta_d, \gamma_d]$, and the FRD normalization rotation angle ϕ_d.

6. **Initial aircraft pose estimate**
The initial aircraft pose estimate, in which ambiguity problems are ignored, is denoted $[\alpha, \beta, \gamma]$. This initial pose estimate is equal to $[\alpha_d, \beta_d, \gamma_d - \phi_d + \phi_{in}]$.

7. **Generate alternative pose estimates**
From the basic pose estimate $[\alpha, \beta, \gamma]$, a number of alternative pose hypotheses are derived to account for the ambiguity that is induced by the object symmetry and the mapping from 3D object to 2D image. The causes of pose ambiguity and the related pose equivalence relations are summarized in table 1. The aircraft pose hypotheses that are generated in processing step 7 are listed in table 2.

Table 1. Causes of object pose ambiguity

Equivalence relation	Cause
$[\alpha,\beta,\gamma] \leftrightarrow [-\alpha,-\beta,\gamma-180°]$	Rotation symmetry (180°) relative to aircraft main body axis
$[\alpha,\beta,\gamma] \leftrightarrow [180°-\alpha,-\beta,\gamma]$	Mirror symmetry relative to the plane through main body axis and tail wing

Table 2. Four aircraft pose hypotheses, based on the initial pose estimate $[\alpha, \beta, \gamma]$

azimuth	elevation	Roll
α	β	γ
$180°-\alpha$	$-\beta$	γ
$180°-\alpha$	$\beta-180°$	γ
α	$-\beta-180°$	γ

8. **Select pose estimate**
   The four pose hypotheses that were generated in step 7 are compared to the previous pose estimate, using a quaternion based pose similarity measure. The best matching hypothesis is considered to be the current pose estimate.

4. SIMULATIONS

In this section we present the results from simulations that were carried out to study the relationship between pose estimation accuracy and parameter settings in the FRD based pose estimation algorithm. In addition a comparison is made between FRD based and moment based pose estimation. Finally, the use of the FRD based pose estimation algorithm in target recognition applications is studied.

1. Data sets

Each pose estimation experiment relies on two different data sets: the feature vector *reference set* is used to fill the algorithm database, while the *test set* contains the images to which the pose estimation algorithm is applied. Both the feature vector reference set and the test set are derived from a source set of synthetic images that show an aircraft from various aspect angles. The source set covers azimuth angles in the range from 0° through 360° and elevation angles in the range from -90° through 90°. In both dimensions samples are taken at 5° intervals, resulting in a total number of 36x72 images. The resolution of the images in the source set is 100x100 pixels. The relation between aspect angle and aircraft image is illustrated in figure 3. The roll angle of the aircraft is zero in the reference feature vector set. In most experiments the test set images are rotated 80° counter clockwise relative to the reference set images. In those experiments where test images with different roll angles are used, this is explicitly stated. To obtain fair test conditions, a leave-one-out method is used that ensures that test and reference set do not have any element in common.

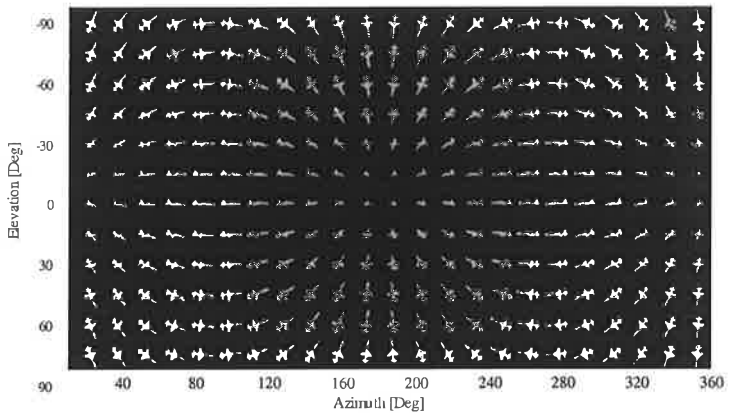

Figure 3. Gray scale images of fighter aircraft for various values of azimuth and elevation

2. Object pose dissimilarity

The relation between two object poses can be uniquely described by a single rotation about a suitable chosen rotation axis. The rotation axis is chosen such that the rotation angle α is minimized. We define the dissimilarity of two object poses P and P' to be equal to the rotation angle α. This concept is illustrated in figure 4

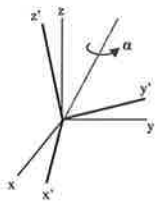

Figure 4. Pose similarity based on an single rotation angle.

3. Resolution dependent pose estimation accuracy

The average pose estimation error that occurred in the FRD based algorithm was evaluated through simulation at six different input image resolutions. In addition a comparison was made to pose estimation results obtained by using a moment based estimation method[3,4]. It should be noted that all pose estimation accuracy measurements are based on the previously defined quaternion based pose difference measure. The outcomes of the simulations indicate that the pose estimation error in the output from the FRD based algorithm is approximately 5° smaller than the pose estimation error in the output of the moment based algorithm. The pose estimation errors of both algorithms are nearly independent of the image resolution for input images in the range between 35% and 100% of the original image resolution.

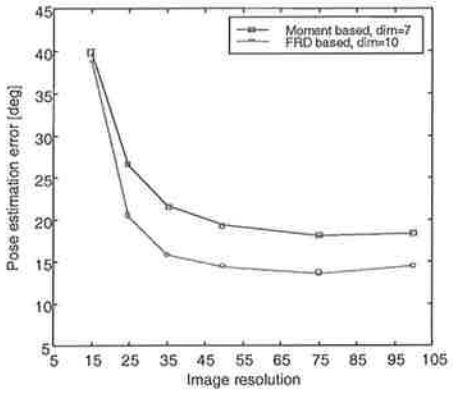

Figure 5. Pose estimation errors of FRD and moment based pose estimation algorithms at six different input image resolutions. Pose estimation errors are measured conform definition II.

5. TEST FLIGHT RESULTS

In November 1997 a measurement campaign was carried out in which several aircraft flights were recorded by cameras and inertial orientation sensors. From these experiments an image sequence, that shows several interesting manoeuvres, was selected for further analysis. The trajectory that was flown by the aircraft is visualised in figure 6 though a ribbon structure in which twists represent aircraft roll manoeuvres.

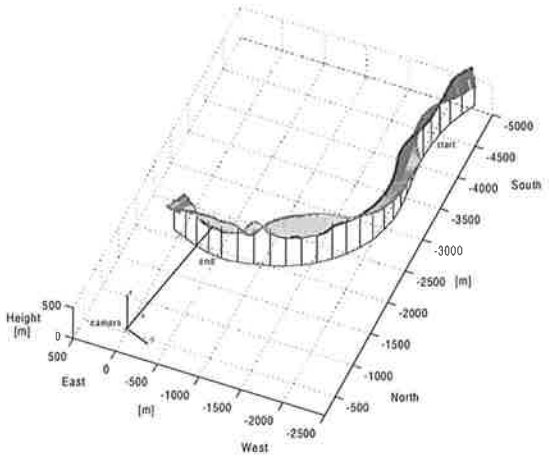

Figure 6. Visualisation of fighter aircraft test flight that was used for measuring pose estimation performance. The bending ribbon indicates aircraft manoeuvres

4. Results

In this paragraph an assessment of pose estimation accuracy, based on comparison of estimated and measured aircraft pose angles, is presented. Aircraft pose angles are expressed relative to a local earth tangent coordinate system. The pose estimation accuracy measurements are based on a quaternion metric. Figure 7 shows a comparison of raw aircraft angle measurements and estimated aircraft angles.

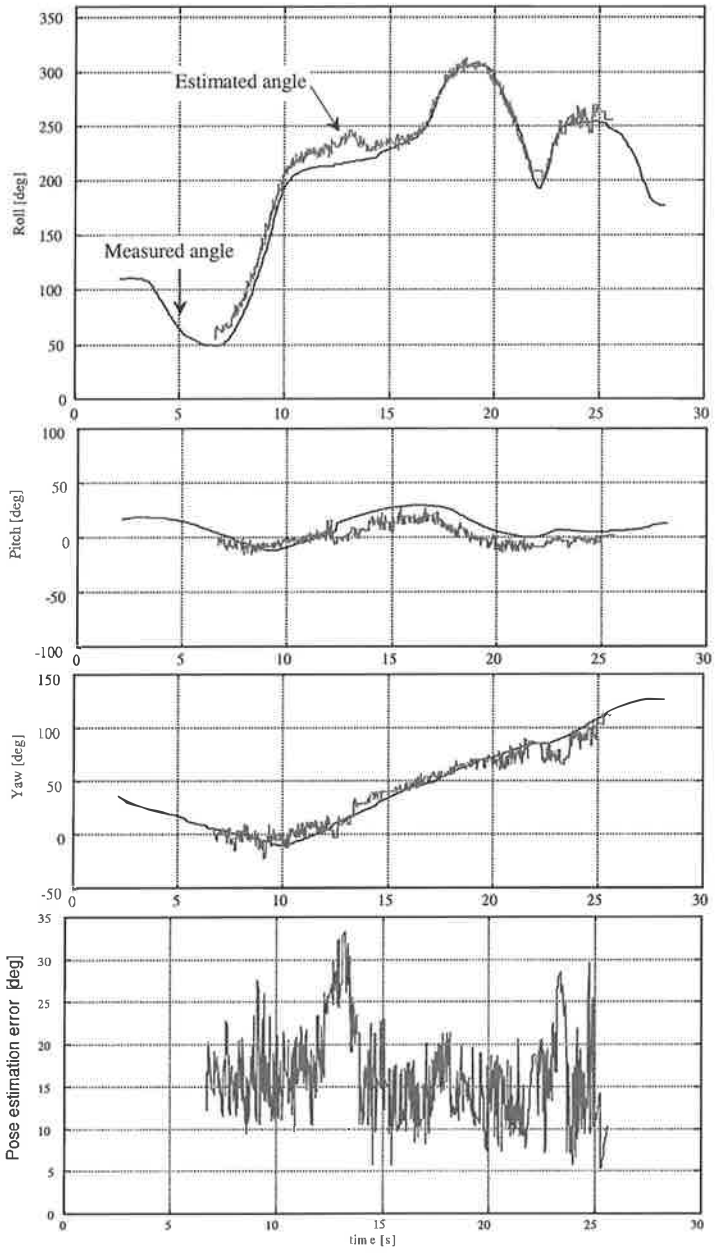

Figure 7. Comparison of raw measured aircraft pose angles and estimated aircraft pose angles.

From the previous graphs it is clear that some artefacts are present in the inertial instrument based aircraft pose data. The step of approximately 7° in the pitch angle that occurs at t≈12s is considered to be such an artefact. Visualisation of the adjusted aircraft angle measurements in synthetic images clearly shows a better agreement when compared to the original

camera video sequence. The original pitch angle measurements and the adjusted pitch angle measurements are compared to the estimated pitch angles in figure 8.

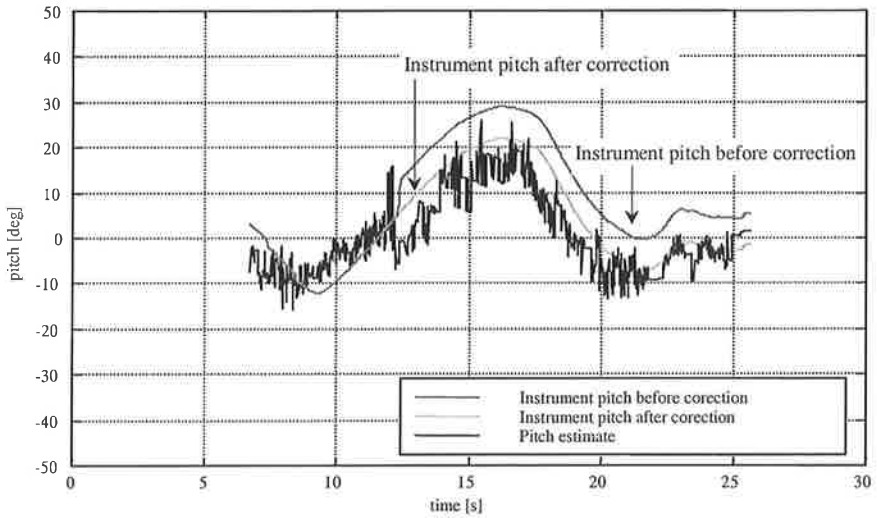

Figure 8. Comparison of raw measured aircraft pitch angles, adjusted measured aircraft pitch angles, and estimated aircraft pitch angles.

A comparison of pose estimation errors, based on adjusted instrument data and raw instrument data is shown in figure 9.

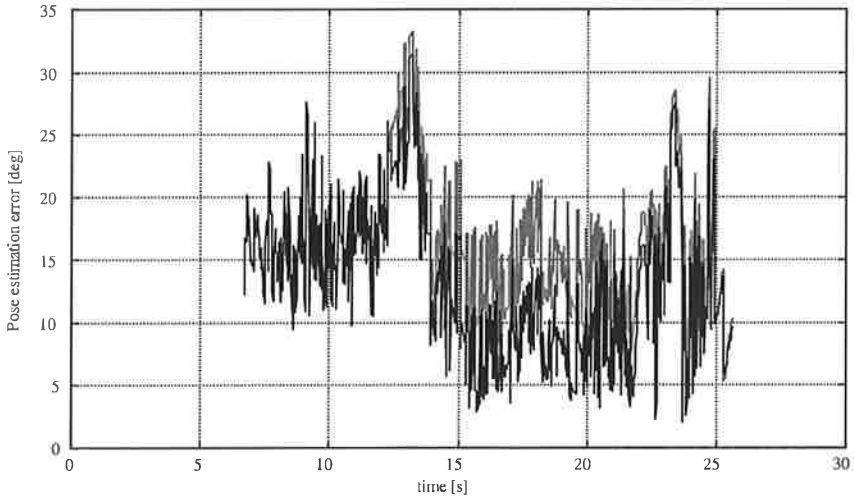

Figure 9. Pose estimation error based on comparison between estimated aircraft pose and raw measurements of aircraft pose (grey), and comparison between estimated aircraft pose and adjusted measurements of aircraft pose (black).

A quantitative comparison of pose estimation errors, based on adjusted instrument data and raw instrument data is shown in table 3.

Table 3. Pose estimation error based on raw pose measurements and adjusted pose measurements.

	Mean pose estimation error	
	(all samples)	(last 500 samples)
Raw angle measurements	16.1821	14.5210
Adjusted angle measurements	13.3264	10.3078

It should be noted that the pose estimation algorithm output is based on trustworthy estimates. This means that pose estimate changes in successive estimates that exceed a certain threshold are disregarded and replaced by the most recent trustworthy estimate. A comparison of pose estimation errors based on trustworthy estimates and pose estimation errors based on all algorithm internal estimates is shown in figure 10.

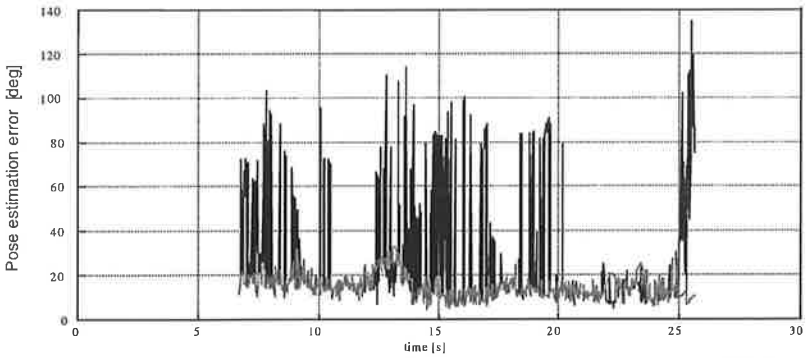

Figure 10. Comparison of raw pose estimation error (black), and pose estimation error after outlier removal (grey).

The ratio between the total number of processed images and the number of images in which outliers had to be removed amounts to 299 / 947 = 1/3. A pose estimate is considered to be an outliner if it difference relative to the previous correct estimate amount to more than 15°.

6. SUMMARY AND CONCLUSIONS

An algorithm was designed and implemented to study the performance that can be achieved in automatic image based aircraft pose estimation. The results from simulations indicate that the FRD based pose estimation algorithm works fairly well down to low resolution images of 35x35 pixels, resulting in a median pose estimation accuracy better than 15°. The evaluation of the pose estimation algorithm with real-world flight data produced an average pose estimation error of 13.3°. Based on these data, we come to the conclusion that the pose error estimates that were obtained from simulations are in good agreement with the results from real-world experiments.

ACKNOWLEDGEMENTS

The author is grateful for the fruitful discussions with N. de Reus, P. Ockeloen, K. Schutte, and B. van den Broek.

REFERENCES

1. D. Sworder and R. Hutchens, "Manoeuvre estimation using measurements of orientation", *IEEE Transactions on Aerospace and Electronic Systems*, vol. 26, no. 4, July 1990.
2. J.D. Kendrick, *Estimation of aircraft target motion using pattern recognition orientation measurements*, Ph.D. dissertation, Air force Inst. Technology, Wright-Patterson Air Force, OH, 1978.
3. M. Breuers, "Image-based aircraft pose estimation using moment invariants", *Proc. of SPIE*, vol 3718, pp. 294-304, 1999.
4. S.A. Dudani, K.J. Breeding and R.B. McGhee, "Aircraft identification by moment invariants", *IEEE Trans. Comput.* C-26, pp. 39-46, 1977.
5. T.P. Wallace and P. Wintz, "An efficient three-dimensional aircraft recognition algorithm using normalised Fourier descriptors", *Comput. Graphics Image Process,* vol. 13, pp. 99-126, 1980.